INCREASED COLLAGEN CROSS-LINKING IS A SIGNATURE OF DYSTROPHIN-DEFICIENT MUSCLE

LUCAS R. SMITH, PhD,[1,2] DAVID W. HAMMERS, PhD,[1,2,3,4] H. LEE SWEENEY, PhD,[1,2,3,4] and ELISABETH R. BARTON, PhD[2,4,5]

[1] Department of Physiology, Perelman School of Medicine, University of Pennsylvania, Philadelphia, Pennsylvania, USA
[2] Pennsylvania Muscle Institute, Perelman School of Medicine, University of Pennsylvania, Philadelphia, Pennsylvania, USA
[3] Department of Pharmacology & Therapeutics, College of Medicine, University of Florida, Gainesville, Florida, USA
[4] Myology Institute, University of Florida, Gainesville, Florida, USA
[5] Department of Applied Physiology and Kinesiology, College of Health and Human Performance, University of Florida, 1864 Stadium Road, 124 Florida Gym, Gainesville, Florida 32611, USA

Accepted 23 November 2015

ABSTRACT: *Introduction:* Collagen cross-linking is a key parameter in extracellular matrix (ECM) maturation, turnover, and stiffness. We examined aspects of collagen cross-linking in dystrophin-deficient murine, canine, and human skeletal muscle. *Methods:* DMD patient biopsies and samples from *mdx* mice and golden retriever muscular dystrophy dog samples (with appropriate controls) were analyzed. Collagen cross-linking was evaluated using solubility and hydroxyproline assays. Expression of the cross-linking enzyme lysyl oxidase (LOX) was determined by real-time polymerase chain reaction, immunoblotting, and immunofluorescence. *Results:* LOX protein levels are increased in dystrophic muscle from all species evaluated. Dystrophic mice and dogs had significantly higher cross-linked collagen than controls, especially in the diaphragm. Distribution of intramuscular LOX was heterogeneous in all samples, but it increased in frequency and intensity in dystrophic muscle. *Conclusion:* These findings implicate elevated collagen cross-linking as an important component of the disrupted ECM in dystrophic muscles, and heightened cross-linking is evident in mouse, dog, and man.

Muscle Nerve **54**: 71–78, 2016

There are currently 41 documented forms of muscular dystrophy caused by monogenic mutations.[1] Many result in progressive deterioration of functional musculature and its replacement by noncontractile fibrotic tissue.[2] Duchenne muscular dystrophy (DMD), an X-linked disease caused by disruption of the dystrophin gene, is one of the most common forms, affecting 1 in 4,000 boys.[3] It is characterized by a progressive loss of muscle function.[2] Dystrophin-deficient muscles are vulnerable to contraction-induced damage, which leads to repeated cycles of necrosis and regeneration that result in failed regeneration, increased fibrosis, and progressive loss of muscle function.[2,4] In DMD patients, this results in loss of ambulation, severe muscle contractures, and, without support devices, eventual loss of ventilatory function, leading to premature death.[5,6] Understanding the pathophysiology of the associated fibrosis is critical for identification of novel and optimized therapeutic targets to improve both quantity and quality of life in affected individuals.

Within skeletal muscle, the extracellular matrix (ECM) is dually important for providing a cellular scaffold and transmitting muscle contractile forces.[7,8] However, the pathological accumulation of ECM that occurs in fibrosis impairs normal cell function and force transmission, as well as inhibiting repair and regeneration, thereby compounding the primary cellular defect. The vast majority of research toward countering fibrosis in muscular dystrophy has targeted pathways involved in pathologic collagen production, primarily the transforming growth factor (TGF)-β-Smad2/3 signaling pathway.[9] These strategies may prevent fibrosis, but they may also alter the normal physiologic scaffolding properties of the ECM.

Although increased stiffness is often associated with fibrotic muscles,[10,11] we recently reported that total muscle collagen content does not correlate with tissue stiffness in *mdx* mice.[12] These data suggest that posttranslational modifications of collagen, such as collagen cross-linking, are critical parameters in dystrophic muscle pathology. Fibrillar collagens make up most of the collagen in skeletal muscle and are the primary load-bearing structures within the ECM.[13,14] Fibrillar collagen α-chains form a triple helix that is secreted in a pro-form, cleaved, and cross-linked into non-reducible collagen fibrils. The mechanical strength of collagen fibrils is highly dependent on the extent of cross-link formation.[15]

Abbreviations: BSA, bovine serum albumin; DAPI, 4′,6-diamidino-2-phenylindole; DMD, Duchenne muscular dystrophy; ECM, extracellular matrix; GRMD, golden retriever muscular dystrophy; HRP, horseradish peroxidase; LOX, lysyl oxidase; PCR, polymerase chain reaction; PIF, pepsin-insoluble fraction; PSF, pepsin-soluble fraction; PVDF, polyvinylidene fluoride; SDS-PAGE, sodium dodecylsulfate–polyacrylamide gel electrophoresis; TA, tibialis anterior; TBST, Tris-buffered saline plus Tween 20; TGF, transforming growth factor

Key words: collagen cross-linking; extracellular matrix; fibrosis; lysyl oxidase; muscular dystrophy

L.R.S., D.W.H., and E.R.B. contributed equally to this study.

This study was supported by grants from the National Institute of Arthritis and Musculoskeletal and Skin Diseases (AR-057363 and AR-052646). L.R.S. and D.W.H. were supported by a National Institute of Arthritis and Musculoskeletal and Skin Diseases T32 training grant to the Pennsylvania Muscle Institute (T32-AR-053461) for part of this work.

Correspondence to: E.R. Barton; e-mail: erbarton@ufl.edu

Published online 30 November 2015 in Wiley Online Library (wileyonlinelibrary.com). DOI 10.1002/mus.24998

Collagen is dramatically overexpressed in fibrotic muscle tissue,[10,16] and its content is inversely correlated with muscle strength in dystrophy.[17] Little is known about the extent of posttranslational modifications, including cross-linking in dystrophic muscle. The initial step in collagen cross-linking requires lysyl oxidase (LOX, or family members LOXL1–LOXL4) to prime lysines and hydroxylines on collagen to produce mature pyridinoline cross-links.[18] Extent of LOX expression has been highly associated with tissue fibrosis and stiffness in multiple tissues, including the heart.[19] Indeed, LOX is among the most highly upregulated genes in the myocardium and limb muscle of the *mdx* mouse, a model of DMD.[20] Because cross-linked collagen is more resistant to proteolysis,[21] extensively cross-linked collagen may contribute to irreversible scar formation. Therefore, collagen cross-linking may be a critical factor in determining fibrotic tissue stiffness in contrast to the content of collagen in fibrotic lesions in DMD. The goals of this study were to clarify the association between LOX levels and collagen cross-linking in dystrophic muscle and to determine if indices of heightened cross-linking exist in animal models for DMD and DMD patients.

METHODS

Animals. The University of Pennsylvania Animal Care Committee approved the experiments in this study. Six- and 18-month-old male C57 and *mdx* mice were euthanized, and the tibialis anterior (TA) muscle and the diaphragms were dissected. They were either flash frozen in liquid nitrogen for biochemical analysis or embedded in OCT and frozen in melting isopentane for histological evaluation. Portions of TA and diaphragm were collected from 1-year-old golden retriever muscular dystrophy (GRMD) dogs ($n = 3$) and an unaffected dog ($n = 1$) following unrelated terminal endpoints and were either flash frozen or frozen in OCT. Samples were stored at –80 °C until further analysis.

Human Biopsy Samples. Samples of human quadriceps muscle ($n = 3$) were obtained from the Wellstone Muscular Dystrophy Cooperative Research Center, Tissue and Cell Repository at the University of Iowa, Carver College of Medicine (Iowa City, Iowa). The DMD patients were between 5 and 8 years of age, and control patients between 8 and 13 years of age at the time of biopsy.

Gene Expression Analysis. Total RNA was isolated from murine and canine muscles using TRIzol reagent (Invitrogen) treated with DNase (Promega) and reverse transcribed to cDNA using the GeneAmp RNA polymerase chain reaction (PCR) kit (Applied Biosystems) using the manufacturer's directions. Real-time PCR (Model 7300; Applied Biosystems) was conducted on the resulting cDNA with Power SYBR Green Master Mix (Applied Biosystems). Expression levels of *Lox* (accession numbers: mouse, NM_010728; dog, XM_538599), *Loxl2* (mouse, XM_006519744), and *Col1a2* (mouse, NM_007743; dog, NM_001003187) were determined with 18S expression serving as the reference housekeeping gene.

Immunoblotting. Flash-frozen murine and canine muscle tissue was finely crushed and homogenized in tissue protein extraction reagent (T-PER; Thermo Scientific) supplemented with protease and phosphatase inhibitor cocktails (Thermo Scientific). Quadriceps biopsy samples from healthy males and DMD patients (pooled from 25 10-μm frozen sections from each patient) were lysed in radioimmunoprecipitation assay (RIPA) buffer supplemented with protease and phosphatase inhibitor cocktails (Sigma-Aldrich).

Protein concentration was measured using the Bradford method (Bio-Rad). Samples were separated by sodium dodecylsulfate–polyacrylamide gel electrophoresis (SDS-PAGE) on Tris-HCl-polyacrylamide gels (Bio-Rad) and transferred to polyvinylidene fluoride (PVDF) membranes. Membranes were blocked with 5% milk in Tris-buffered saline and Tween 20 (TBST) and incubated in primary antibody diluted in 2% milk–TBST overnight at 4 °C, using anti-LOX (Abcam ab31238; 1:500) for human and canine samples and anti-LOX (Novus NBP2-24877; 1:500) for mouse samples. The membranes were washed, incubated in anti-rabbit horseradish peroxidase (HRP)–conjugated secondary antibody (Cell Signaling Technologies), and visualized using ECL Plus reagents (Thermo Scientific) and autoradiography film (BioExpress). To provide loading controls, membranes were stripped and either reprobed for glyceraldehyde 3-phosphate dehydrogenase (GAPDH; sc-25778; 1:2,000; Santa Cruz Biotechnology) or stained with Coomassie Blue (Bio-Rad) or Ponceau S (Sigma-Aldrich) solution for visualization.

Collagen Stability. A collagen solubility assay was adapted[22,23] to quantify the proportion of mature cross-linked collagen from non–cross-linked and immature cross-linked collagen. Briefly, flash-frozen muscle tissue was ground using a mortar and pestle over dry ice and then weighed. The tissue was washed in 1 ml of PBS and stirred for 30 minutes at 4 °C before centrifuging at 16,000*g* for 30 minutes at 4 °C. Non–cross-linked collagen was digested in a 1:6 (weight:volume) solution of 0.5 M acetic acid with 1 mg/ml pepsin, stirring overnight at 4 °C. After centrifuging at 16,000*g* for 30 minutes at 4 °C, the supernatant was collected as the pepsin-soluble fraction (PSF), and the pellet was kept as the pepsin-insoluble fraction (PIF). For the PSF, a 1:1 volume of 4 M NaCl was added and stirred for 30 minutes at 4 °C. The PSF was then

centrifuged at 16,000*g* for 30 minutes at 4 °C, and the supernatant was discarded. The collagen contents of the PSF and PIF were then determined by a hydroxyproline assay.

Hydroxyproline Assay. A hydroxyproline assay was performed to quantify collagen content in both the PSF and PIF, as described in previous studies.[12,24] The samples were hydrolyzed overnight in 0.5 ml of 6 M hydrochloric acid at 105 °C. 10 μl of hydrolysate were mixed with 150 μl isopropanol followed by 75 μl of 1.4% chloramine-T (Sigma, St. Louis, Missouri) in citrate buffer and oxidized at room temperature for 10 minutes. The samples were then mixed with 1 ml of a 3:13 solution of Ehrlich reagent [1.5 g of 4-(dimethylamino)benzaldehyde (Sigma), 5 ml ethanol, and 337 μl sulfuric acid] to isopropanol and incubated for 45 minutes at 55 °C. Quantification was determined by extinction measurement of the resulting solution at 558 nm. A standard curve (0–1,000 μM, trans-4-hydroxy-L-proline; Sigma) was included in each assay. Results are reported as micrograms of hydroxyproline per milligram of tissue wet weight.

Picosirius Red Staining. Frozen OCT-embedded GRMD samples were sectioned at 10 μm, and Picosirius red staining was performed as previously described.[12] Briefly, sections were fixed in 4% paraformaldehyde for 10 minutes, rinsed, air dried, stained for 1 hour in 0.1% (wt/vol) Sirius red (Sigma-Aldrich), dissolved in saturated aqueous picric acid (Sigma-Aldrich), washed in 2 changes of 0.5% acetic acid, dehydrated in 3 changes of 100% ethanol, cleared with Citra Solv, and mounted with Cytoseal. The resulting slides were viewed under circularly polarized light scope (DMLP; Leica), rotating polarizer, rotating analyzer, and dual quarter wave plates on a camera system (Micropublisher 5.0; Q Imaging).

Immunofluorescence. Acetone-fixed 10-μm sections of mouse, dog, and patient muscle were incubated overnight at 4 °C with anti-LOX (Abcam ab31238; 1:500) and anti-vimentin (Novus MB300; 1:800) primary antibodies using 5% bovine serum albumin (BSA)–PBS with 0.1% Triton X-100 as a blocking solution/diluent. Alexa 568–conjugated anti-rabbit IgG (Molecular Probes; 1:500) and Alexa 488–conjugated anti-chicken IgY (Jackson; 1:500) secondary antibodies were used. Slides were mounted using VectaShield with 4′,6-diamidino-2-phenylindole (DAPI; Vector Labs) and imaged using the confocal microscope (Model TSC-SP8; Leica). Quantification of human LOX immunoreactivity was achieved by analysis of 5 independent fields of view (20×) from control ($n = 3$) and DMD patient ($n = 3$) quadriceps sections using SMASH muscle image analysis software.[25]

Statistical Analysis. All results are presented as mean ± SEM unless otherwise stated. Statistical analysis of the mouse data was performed by 2-way analysis of variance using genotype and muscle followed by a Bonferroni *post hoc* test comparing genotypes within muscles and muscles within a genotype. For the human samples, a Student *t*-test was used to compare muscles from unaffected to DMD subjects. For the dog samples there was only a single control dog, so only a paired Student *t*-test was performed between muscles of GRMD dogs. $P < 0.05$ was considered statistically significant.

RESULTS

LOX and Collagen Cross-Linking Is Increased in *mdx* Diaphragm. Gene expression of the collagen cross-linking enzyme LOX was evaluated at the ends of the mouse phenotypic spectrum by comparing a less affected limb muscle (TA) and the more severely affected diaphragm muscle of *mdx* mice at age 6 months to age-matched C57 mice (Fig. 1A). Although *Lox* expression was not significantly different between the wild-type and dystrophic TA, it was significantly elevated in the diaphragms of *mdx* mice. Accordingly, *Col1a2* expression was also highly upregulated in the *mdx* diaphragm; however, expression of the LOX family member, *Loxl2*, was unchanged across the samples. At the protein level (Fig. 1B), LOX abundance was similarly increased in the *mdx* diaphragms at age 6 months compared with those of C57 mice and was also significantly higher in the dystrophic TA.

The consequence of higher levels of LOX was evaluated with a collagen solubility assay, where the soluble, insoluble, and total collagen levels were determined in *mdx* and control muscles (Fig. 1C). The amount of soluble collagen, representing non–cross-linked and immature cross-linked collagen, was similar between all muscles analyzed and represented a minor proportion of the total collagen pool. In contrast, 6-month *mdx* diaphragms had significantly more mature cross-linked insoluble collagen and total collagen than the *mdx* TA and age-matched C57 diaphragms. To determine whether there was an age-dependent increase in either LOX or collagen, muscles from 18-month-old *mdx* mice were compared with those from 6-month-old animals. LOX levels were similar between the 2 ages, but the *mdx* diaphragm continued to accrue insoluble collagen (Fig. 1D), whereas the TA insoluble content remained unchanged (data not shown). These data demonstrate that LOX is chronically elevated in the dystrophic mouse diaphragm, which results in progressive accumulation of cross-linked collagen.

Increased Cross-Linking Features in GRMD Muscle. Due to the relatively mild phenotype of the *mdx* mouse compared with DMD patients, we also investigated

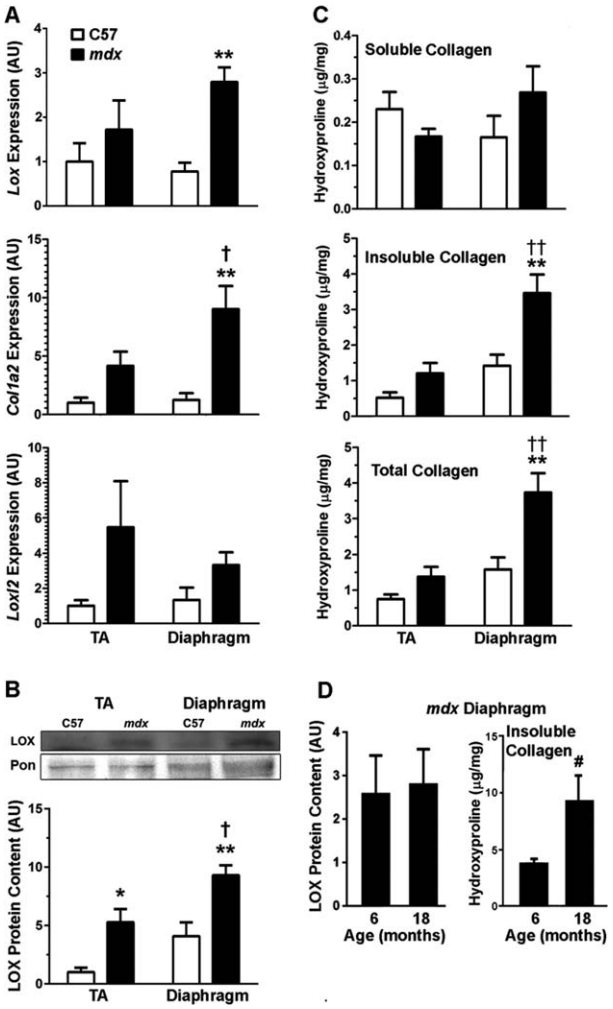

FIGURE 1. *Lox* expression and collagen cross-linking in the *mdx* murine model of DMD. **(A)** *Lox* transcript level is increased in *mdx* muscle ($n = 7$) over control ($n = 6$). *Col1a2* is increased in *mdx* muscles ($n = 7$) over control ($n = 6$), and in *mdx* diaphragm over TA. *Loxl2* tends to be upregulated in *mdx* muscles ($n = 3$) over control ($n = 3$). **(B)** Representative portion of immunoblot for LOX (32 kDa) with Ponceau stain for loading control. LOX protein is increased in *mdx* ($n = 3$) over control ($n = 3$), with *mdx* diaphragm higher than TA. **(C)** Soluble hydroxyproline content, representing non–cross-linked or immature cross-linked collagen, of *mdx* ($n = 6$) muscles are not different from C57 ($n = 6$). Insoluble hydroxyproline content, representing cross-linked collagen, and total collagen are increased in *mdx*, with *mdx* diaphragm higher than control diaphragm or *mdx* TA for both insoluble and total collagen. **(D)** Immunoblot of *mdx* diaphragm for LOX shows no additional increase at 18 months ($n = 2$) compared with 6 months. Insoluble cross-linked collagen is higher at 18 months ($n = 2$) compared with 6 months in *mdx* diaphragm. Significantly different *post-hoc* test, indicated by $^{*}P < 0.05$ and $^{**}P < 0.01$, between genotypes of same muscle; $^{\dagger}P < 0.05$ and $^{\dagger\dagger}P < 0.01$, between muscles of the same genotype; and $^{\#}P < 0.05$, between ages of *mdx* diaphragm.

LOX levels and collagen cross-linking in the more severe GRMD dog model of DMD. Like the *mdx* mouse, GRMD exhibits differential disease severity between limb muscles and the diaphragm. Similar to our findings in the *mdx* mouse, GRMD diaphragm displayed high upregulation of both *LOX* and *COl1A2* gene expression over control dog levels, with no change in the TA (Fig. 2A). LOX protein, although not detectable in control dog samples by Western blotting, was observed in GRMD samples, where its abundance among GRMD diaphragms was consistently higher than the dog-matched TA (Fig. 2B). Accordingly, GRMD diaphragms also contained more insoluble and total collagen than all other samples (Fig. 2C), in agreement with the findings in mice described above.

As previously performed on *mdx* mouse muscle,[12] the collagen density of GRMD muscle sections was

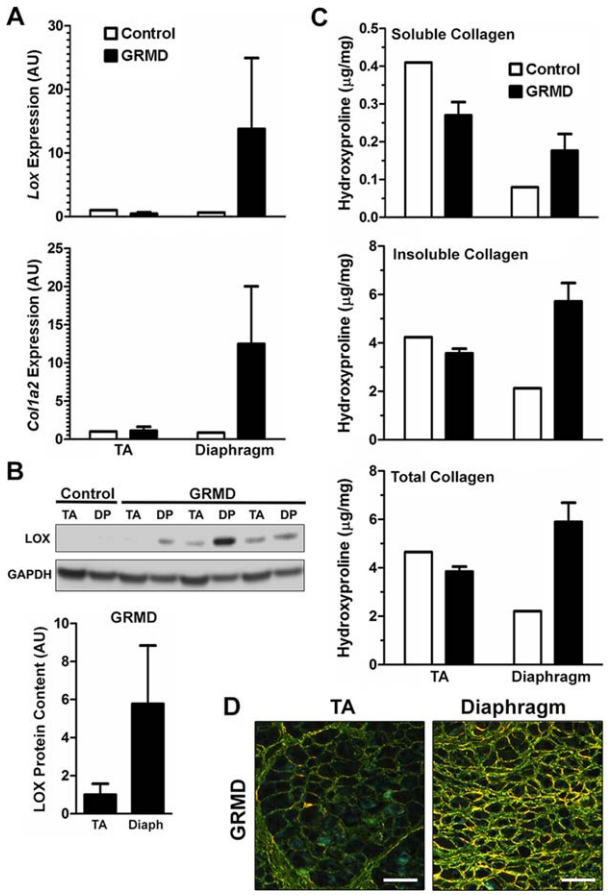

FIGURE 2. *LOX* expression and collagen cross-linking in the GRMD dog model of DMD in limb and diaphragm muscle. **(A)** Transcriptional level of *LOX* and *COL1A2* are dramatically increased in GRMD diaphragm. **(B)** Immunoblot for LOX (32 kDa) using GAPDH (37 kDa) as a loading control from wild-type and GRMD dogs. Protein level of LOX is not observable in wild-type dogs, but is present in GRMD muscles, with diaphragm consistently higher than dog matched TA. **(C)** Soluble hydroxyproline content, representing non–cross-linked collagen or immature cross-linked collagen, does not show a consistent difference between wild-type and GRMD. Insoluble hydroxyproline content, representing cross-linked collagen, is highest in the GRMD diaphragm. Total collagen content is highest in the GRMD diaphragm. Data are from 3 GRMD dogs and 1 control dog. **(D)** Representative images of GRMD dog TA and diaphragm muscles viewed under circularly polarized light. Birefringent fibrillar collagen is visible with loosely (green), moderately (yellow), and densely (red) packed collagen. Scale bar = 50 μm.

visualized under circularly polarized light (Fig. 2D). In accordance with the biochemical data described above, the GRMD TA contained mostly loosely packed collagen bundles (visualized as green), with an extensive perimysial layer, whereas the diaphragm collagen bundles were largely intermediate (yellow) or densely (orange to red) packed, verifying that collagen density is increased in GRMD diaphragm compared with limb muscle. It is also notable that, in the GRMD diaphragm, unlike the TA, the robust endomysial expansion resulted in a lack of distinction between endomysial and perimysial stromal regions. Thus, the canine model of DMD also displays heightened indices of collagen cross-linking in the diaphragm as compared with less affected limb muscle.

LOX Localization Is Altered in Dystrophic Muscle. LOX cross-linking activity occurs in the ECM, but many different cell types can produce this enzyme, including fibroblasts and muscle fibers.[19,26–28] To determine the distribution of excess LOX in dystrophic muscle, immunofluorescence of LOX and vimentin, a marker of mesenchemyl cells, including fibroblasts, was performed. In healthy muscle, LOX was evident in sparse puncta associated with the ECM. For the mouse diaphragm, these areas were observed along the epimysium and also in small foci in the perimysium and perivascular areas (Fig. 3A and B). Approximately 2–5 LOX-positive regions were observed per cross-section. The same infrequent LOX locations were observed in the wild-type mouse TA (data not shown). For the diaphragm of an unaffected dog (Fig. 3C) the trend was similar. Of particular interest were muscle fibers that were positive for LOX both inside and outside of the sarcolemma, suggesting that the muscle fiber itself was producing LOX (Fig. 3C, inset). Dystrophic muscles from both species exhibited similar LOX "hot spots," but these were more extensive both in number and in size (Fig. 3D). This included more pronounced distribution of LOX along the endomysium, evident in the *mdx* TA muscle. Taken together, the expanded distribution of LOX in *mdx* and GRMD muscle sections was consistent with the increased LOX transcript and protein levels found in dystrophic muscles.

LOX is Increased in DMD Patient Muscle. To substantiate the translational value of our animal model data, we measured LOX protein in quadriceps biopsy samples from unaffected control subjects and DMD patients by Western blotting (Fig. 4A). LOX protein abundance was increased 3-fold in DMD samples. Similar to the mouse and dog tissue, immunofluorescence of unaffected control human muscle demonstrated infrequent LOX-positive loci, which were primarily located near the perimysial regions (Fig. 4B). In DMD tissue, LOX again had a broader distribution that included more frequent foci observed in both endomysial and perimysial regions. Quantification of the LOX-positive area

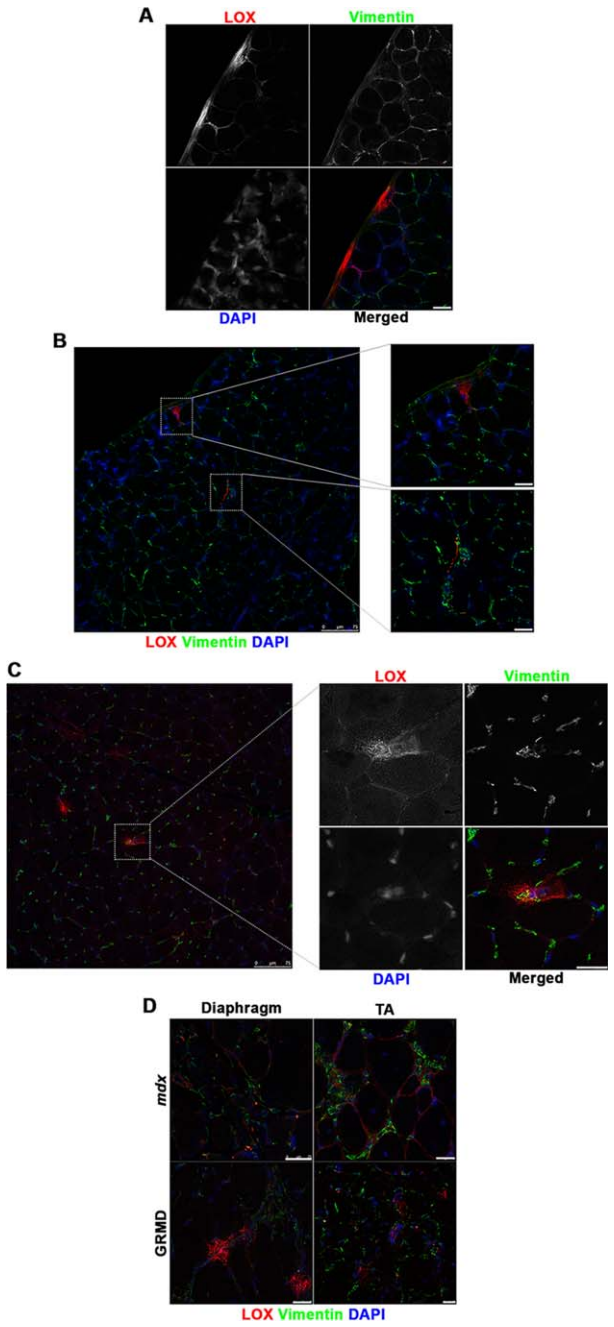

FIGURE 3. Confocal microscopic immunofluorescent images of lysyl oxidase (LOX; red), vimentin (green), and DAPI (blue) on 10-μm-thick cryosections. **(A)** C57 mouse diaphragm shows epimysial focal regions of LOX as well as **(B)** perimysial regions of focal LOX, shown in insets. **(C)** Unaffected dog diaphragm demonstrates similar focal expression of LOX as C57 mice. **(D)** Diaphragm and tibialis anterior (TA) samples from *mdx* mice and GRMD dogs depict increased frequency of focal LOX regions and endomysial LOX. Higher magnification outsets of **(B)** and **(C)** are indicated by dotted square regions of the lower magnification image. Scale bars = 25 μm, unless indicated otherwise.

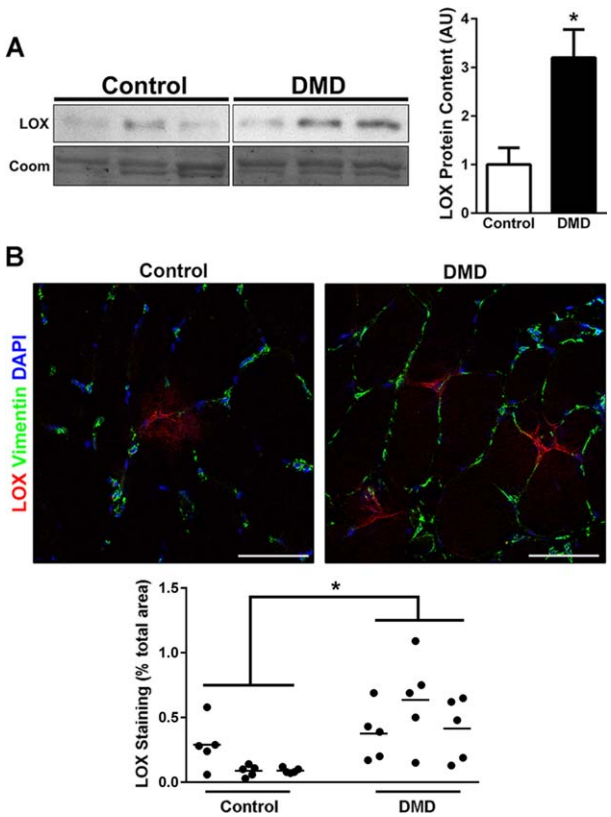

FIGURE 4. LOX in human DMD patients. **(A)** Immunoblot for LOX (32 kDa) using Coomassie staining as a loading control from quadriceps biopsies of control ($n = 3$) and DMD ($n = 3$) patients. All lanes are on the same blot with intervening lanes excluded. Quantification of LOX blots from human patients indicates a significant increase in LOX expression of DMD patients compared with unaffected controls. **(B)** Immunofluorescent confocal microscopy images of lysyl oxidase (LOX; red), vimentin (green), and DAPI (blue) on 10-μm-thick cryosections from human quadriceps muscle. Unaffected control muscle shows infrequent LOX foci relative to DMD muscle. Area fractions are quantified showing 5 regions of interest (circles) from each subject biopsy with averages (lines) from DMD ($n = 3$) and control ($n = 3$) patients, demonstrating significantly increased LOX staining in DMD muscle. Significant difference indicated by $^*P < 0.05$ for LOX expression between human patient groups. Scale bar, 50 μm.

fraction confirmed our Western blotting results, with a 3-fold increase compared with control subjects. These data demonstrate that the muscles of DMD patients have increased LOX content and distribution, likely contributing to the progressive fibrotic replacement of muscle.

DISCUSSION

Skeletal muscle fibrosis is an excessive deposition of ECM components and accompanies the chronic damage that occurs in muscular dystrophy. Little is known about how this aberrant ECM is organized in fibrotic dystrophic muscle, but there is evidence that posttranslational modification of the ECM may be part of the dystrophic pathology. Previous measurements of a rarely used chicken model of muscular dystrophy have shown increased proportions of high-molecular-weight collagen suggestive of increased cross-linking.[29] In addition, studies using *mdx* mice demonstrated increased *Lox* expression in heart and limb muscle[20] and histological association between LOX and fibrosis.[17] We have now extended these observations to show that LOX protein is increased in DMD patient muscle, as well as in mouse and dog DMD models. In dystrophic mouse and dog diaphragm, where pathology is the most severe,[10] there is also more collagen cross-linking, as demonstrated by the increased insoluble fraction of collagen. Importantly, there was no increase in LOX with age. Insoluble collagen content increased progressively in the *mdx* diaphragm, demonstrating the negative implications of chronic LOX elevation. We also demonstrated that the increase in LOX is conserved across species with muscular dystrophy. Taken together, we conclude that increased LOX leads to extensive collagen cross-linking, which is an important feature of DMD muscle.

Although the *mdx* mouse is the most commonly studied model of DMD, it does not typically develop fibrosis in the limbs at a young age, and it has several differences from the human disease.[4,30] Lifespan is only moderately affected in the *mdx* mouse, and, although limb muscles undergo cycles of degeneration and regeneration, there is relatively little fibrosis. The *mdx* diaphragm most accurately reflects the muscle pathology observed in DMD patients,[10] thus it is not surprising that our measurements of cross-linking were also most prominent in the *mdx* diaphragm compared with the TA muscles. This is consistent with our previous observations of increased collagen packing density in the *mdx* diaphragm.[12] To determine whether our results were consistent in a model that more accurately exhibits features of DMD, we used the GRMD dog model.[31] GRMD dogs also exhibit increased cross-linked collagen and increased LOX levels, supporting collagen cross-linking as a major feature of the disease that is maintained across species. However, increased cross-linking was not evident in the GRMD TA muscles. Part of the reason we could not detect this difference, as one would expect for larger mammals, is the presence of a very thick perimysium layer that is found in both unaffected healthy and dystrophic dog TA muscles. This layer is an important structural component of limb muscles in dogs and is cross-linked to a greater extent than the rest of the ECM in this muscle. Consistent with this is the localization of more densely packed collagen within the TA perimysium compared with the endomysium. As such, the collagen solubility measurements of muscle homogenates where the perimysium is the overwhelmingly dominant source of matrix likely masks the changes that may have occurred in the endomysial layer around the fibers. In contrast,

the GRMD diaphragm possessed more densely packed collagen fibrils throughout the muscle, which was accompanied by an increase in collagen insolubility.

To verify that the elevation of LOX observed in animal models is also a feature of DMD, human biopies were examined. In agreement with the animal models, LOX expression was shown to be elevated in quantity as well as in frequency of "hot spots" with high focal expression. This is also consistent with 3 published microarray studies in the Gene Expression Omnibus database,[32] which showed significant upregulation of LOX in DMD ($P = 4.9 \times 10^{-7}$, GDS214[33]; $P = 6.8\ 10^{-4}$, GDS3027[34]; $P = 4.7 \times 10^{-2}$, GDS563[35]. Although we were not able to measure collagen cross-linking in human samples directly, the increased LOX levels suggest that muscle in DMD is more extensively cross-linked as observed in animal models.

Collagen cross-linking has been described as a major factor in fibrosis of multiple tissues,[36,37] including the heart.[38] The role of collagen cross-linking in the heart is of great clinical significance in patients with DMD, as it also undergoes a fibrotic response. Whereas *Lox* mRNA is known to be increased in *mdx* cardiac muscle,[20] LOX protein levels and collagen cross-linking have not been studied but should be a target of future investigation. Increased collagen cross-linking is thought to lead to a stiffer ECM and tissue, as demonstrated in the left ventricle of the fibrotic heart.[38] However, recent reports of muscle stiffness in *mdx* mice have shown relatively more stiffening of limb muscle as opposed to the diaphragm,[12] even though cross-linking is most prevalent in the diaphragm. Collagen content shows little correlation with passive stiffness,[12] but collagen cross-linking does not account for additional variability in muscle fiber bundle stiffness.[39] This suggests that, although collagen may be stiffer at the molecular level, other parameters of collagen organization dictate muscle stiffness at the tissue level. However, this does not preclude the micro-stiffness of the cross-linked collagen fibrils from playing a critical role in the cellular response to collagen cross-linking in fibrosis. LOX is critical to the integrity of the developing diaphragm, as mice that lack *LOX* often die perinatally from diaphragmatic hernias.[40] Further, skeletal muscle development is disrupted in *LOX* knockout mice independent of skeletal or tendon defects, demonstrating a role for LOX in this process.[28] LOXL1–LOXL4 are also capable of cross-linking collagen, but little is known about their expression in muscle. The LOXL1–LOXL4 family members have a conserved domain responsible for catalyzing the initial reaction in collagen cross-linking. Their distinct roles are not well understood, but LOXL2 has been shown to be upregulated in fibrotic tissue and responsible for collagen cross-linking in fibrosis.[37] Our initial investigation showed that LOXL2 expression is not significantly altered in dystrophic muscle, providing supporting evidence for LOX being the primary enzyme responsible for cross-linking changes in dystrophic muscle. Critically, it is well established that cross-linked collagen is much less susceptible to turnover,[21] thus implicating collagen cross-linking in the development of progressive scar tissue formation that predominates in muscles from DMD patients.

LOX is known to be produced by vascular cells, including endothelial cells,[26] smooth muscle,[19] and fibroblasts,[27] which are all muscle resident cells; however, a recent report by Kutchuk *et al.* suggested skeletal muscle is also a major contributor of LOX expression, in which myofiber LOX secretion is a negative feedback switch for stromal collagen production and TGF-β activity.[28] Although evidence of LOX production from a specific cell type was not conclusive in our study, we observed scattered stromal foci of LOX immunoreactivity throughout muscle cross-sections, as well as evidence of staining within muscle fibers. In healthy muscle, these foci are typically localized to perimysial and epimysial regions, which are points of high mechanical stress in contracting muscle. The increased frequency and intrafascicular presence of LOX staining in dystrophic muscle could be due to the increased mechanical burden experienced by dystrophin-deficient muscle fibers from reduced attachment to the ECM. Taken together, these lines of evidence suggest LOX secretion into the ECM region is likely regulated by myofiber mechanical sensing, which leads to appropriate ECM adaptation to stress stimuli in non-pathological situations. Unfortunately, dystrophic muscle fibers are impaired in their attachment to the ECM independent of the extent of ECM accumulation and/or cross-linking, thereby preventing the shutdown of collagen and LOX production. This scenario potentially results in continuous endomysial ECM accumulation, which leads to replacement of functional muscle with fibrosis, as seen in DMD patients.[41]

These studies raise important questions regarding the best therapeutic targets for fibrosis. If LOX is critical for reducing TGF-β actions, then targeting it may cause rampant collagen production and lead to increased fibrosis. However, if excessive LOX activity on ECM collagen cross-linking is detrimental to muscle function, then LOX inhibition may be beneficial to diseased muscles where reduced stiffness may also lessen structural damage to muscle fibers. Clinically, therapies that target

LOX and LOX family member activity show promise in preventing lung and liver fibrosis[37] and set a precedent for trials to counter muscle fibrosis using this strategy. However, the balance between the extent of fibrosis and the proportion of cross-linking is a major consideration with respect to the therapeutic window for treatments. Because cross-linked collagen is relatively stable and refractory to remodeling,[18] anti-fibrotic therapies may not remove cross-linked collagen, yet they may gradually reduce overall levels of fibrosis. This could be important if anti-fibrotic therapies are applied to late-stage disease patients in whom considerable cellular loss has occurred in the heart and diaphragm. At that disease stage, removal of all fibrosis could lead to herniation of the diaphragm and aneurysms in the heart, both lethal consequences. In that case, the cross-linked collagen would safeguard against these potentially life-threatening events.

The authors thank Dr. Min Liu and Zuozhen Tian from the Physiological Assessment Core at the University of Pennsylvania. We also acknowledge Dr. Steven Moore from the Wellstone Muscular Dystrophy Cooperative Research Center for providing human biopsies, and Dr. Margaret Sleeper from the Department of Small Animal Clinical Sciences, University of Florida College of Veterinary Medicine, for providing dog tissue.

REFERENCES

1. Kaplan JC, Hamroun D. The 2014 version of the gene table of monogenic neuromuscular disorders (nuclear genome). Neuromuscul Disord 2013;23:1081–1111.
2. Emery AE. The muscular dystrophies. Lancet 2002;359:687–695.
3. Bradley D, Parsons E. Newborn screening for Duchenne muscular dystrophy. Sem Neonatol 1998;3:27–34.
4. Kharraz Y, Guerra J, Pessina P, Serrano AL, Munoz-Canoves P. Understanding the process of fibrosis in Duchenne muscular dystrophy. Biomed Res Int 2014;2014:965631.
5. Kornegay JN, Childers MK, Bogan DJ, Bogan JR, Nghiem P, Wang J, *et al.* The paradox of muscle hypertrophy in muscular dystrophy. Phys Med Rehabil Clin N Am 2012;23:149–172, xii.
6. Smith LR, Lee KS, Ward SR, Chambers HG, Lieber RL. Hamstring contractures in children with spastic cerebral palsy result from a stiffer extracellular matrix and increased in vivo sarcomere length. J Physiol 2011;589:2625–2639.
7. Lieber RL, Ward SR. Cellular mechanisms of tissue fibrosis. 4. Structural and functional consequences of skeletal muscle fibrosis. Am J Physiol Cell Physiol 2013;305:C241–252.
8. Ramaswamy KS, Palmer ML, van der Meulen JH, Renoux A, Kostrominova TY, Michele DE, *et al.* Lateral transmission of force is impaired in skeletal muscles of dystrophic mice and very old rats. J Physiol 2011;589:1195–1208.
9. Burks TN, Cohn RD. Role of TGF-beta signaling in inherited and acquired myopathies. Skelet Muscle 2011;1:19.
10. Stedman HH, Sweeney HL, Shrager JB, Maguire HC, Panettieri RA, Petrof B, *et al.* The mdx mouse diaphragm reproduces the degenerative changes of Duchenne muscular dystrophy. Nature 1991;352:536–539.
11. Hakim CH, Grange RW, Duan D. The passive mechanical properties of the extensor digitorum longus muscle are compromised in 2- to 20-mo-old mdx mice. J Appl Physiol 2011;110:1656–1663.
12. Smith LR, Barton ER. Collagen content does not alter the passive mechanical properties of fibrotic skeletal muscle in mdx mice. Am J Physiol Cell Physiol 2014;306:C889–898.
13. Lund DK, Cornelison DD. Enter the matrix: shape, signal and superhighway. FEBS J 2013;280:4089–4099.
14. Gillies AR, Lieber RL. Structure and function of the skeletal muscle extracellular matrix. Muscle Nerve 2011;44:318–331.
15. Avery NC, Bailey AJ. Enzymic and non-enzymic cross-linking mechanisms in relation to turnover of collagen: relevance to aging and exercise. Scand J Med Sci Sports 2005;15:231–240.
16. Zhu J, Li Y, Shen W, Qiao C, Ambrosio F, Lavasani M, *et al.* Relationships between transforming growth factor-beta1, myostatin, and decorin: implications for skeletal muscle fibrosis. J Biol Chem 2007;282:25852–25863.
17. Desguerre I, Mayer M, Leturcq F, Barbet JP, Gherardi RK, Christov C. Endomysial fibrosis in Duchenne muscular dystrophy: a marker of poor outcome associated with macrophage alternative activation. J Neuropathol Exp Neurol 2009;68:762–773.
18. Yamauchi M, Shiiba M. Lysine hydroxylation and crosslinking of collagen. Methods Mol Biol 2002;194:277–290.
19. Rodriguez C, Martinez-Gonzalez J, Raposo B, Alcudia JF, Guadall A, Badimon L. Regulation of lysyl oxidase in vascular cells: lysyl oxidase as a new player in cardiovascular diseases. Cardiovasc Res 2008;79:7–13.
20. Spurney CF, Knoblach S, Pistilli EE, Nagaraju K, Martin GR, Hoffman EP. Dystrophin-deficient cardiomyopathy in mouse: expression of Nox4 and Lox are associated with fibrosis and altered functional parameters in the heart. Neuromuscul Disord 2008;18:371–381.
21. Eyre DR, Paz MA, Gallop PM. Cross-linking in collagen and elastin. Annu Rev Biochem 1984;53:717–748.
22. Babraj JA, Cuthbertson DJ, Smith K, Langberg H, Miller B, Krogsgaard MR, *et al.* Collagen synthesis in human musculoskeletal tissues and skin. Am J Physiol Endocrinol Metab 2005;289:E864–869.
23. Matmaroh K, Benjakul S, Prodpran T, Encarnacion AB, Kishimura H. Characteristics of acid soluble collagen and pepsin soluble collagen from scale of spotted golden goatfish (*Parupeneus heptacanthus*). Food Chem 2011;129:1179–1186.
24. Heydemann A, Huber JM, Demonbreun A, Hadhazy M, McNally EM. Genetic background influences muscular dystrophy. Neuromuscul Disord 2005;15:601–609.
25. Smith LR, Barton ER. SMASH—semi-automatic muscle analysis using segmentation of histology: a MATLAB application. Skelet Muscle 2014;4:21.
26. Alcudia JF, Martinez-Gonzalez J, Guadall A, Gonzalez-Diez M, Badimon L, Rodriguez C. Lysyl oxidase and endothelial dysfunction: mechanisms of lysyl oxidase down-regulation by pro-inflammatory cytokines. Front Biosci 2008;13:2721–2727.
27. Voloshenyuk TG, Landesman ES, Khoutorova E, Hart AD, Gardner JD. Induction of cardiac fibroblast lysyl oxidase by TGF-beta1 requires PI3K/Akt, Smad3, and MAPK signaling. Cytokine 2011;55:90–97.
28. Kutchuk L, Laitala A, Soueid-Bomgarten S, Shentzer P, Rosendahl AH, Eilot S, *et al.* Muscle composition is regulated by a Lox-TGFbeta feedback loop. Development 2015;142:983–993.
29. Feit H, Kawai M, Mostafapour AS. The role of collagen crosslinking in the increased stiffness of avian dystrophic muscle. Muscle Nerve 1989;12:486–492.
30. Desguerre I, Arnold L, Vignaud A, Cuvellier S, Yacoub-Youssef H, Gherardi RK, *et al.* A new model of experimental fibrosis in hindlimb skeletal muscle of adult mdx mouse mimicking muscular dystrophy. Muscle Nerve 2012;45:803–814.
31. Valentine BA, Cooper BJ, de Lahunta A, O'Quinn R, Blue JT. Canine X-linked muscular dystrophy. An animal model of Duchenne muscular dystrophy: clinical studies. J Neurol Sci 1988;88:69–81.
32. Edgar R, Domrachev M, Lash AE. Gene Expression Omnibus: NCBI gene expression and hybridization array data repository. Nucleic Acids Res 2002;30:207–210.
33. Chen YW, Zhao P, Borup R, Hoffman EP. Expression profiling in the muscular dystrophies: identification of novel aspects of molecular pathophysiology. J Cell Biol 2000;151:1321–1336.
34. Pescatori M, Broccolini A, Minetti C, Bertini E, Bruno C, D'Amico A, *et al.* Gene expression profiling in the early phases of DMD: a constant molecular signature characterizes DMD muscle from early postnatal life throughout disease progression. FASEB J 2007;21:1210–1226.
35. Haslett JN, Sanoudou D, Kho AT, Bennett RR, Greenberg SA, Kohane IS, *et al.* Gene expression comparison of biopsies from Duchenne muscular dystrophy (DMD) and normal skeletal muscle. Proc Natl Acad Sci USA 2002;99:15000–15005.
36. Clarke DL, Carruthers AM, Mustelin T, Murray LA. Matrix regulation of idiopathic pulmonary fibrosis: the role of enzymes. Fibrogenesis Tissue Repair 2013;6:20.
37. Barry-Hamilton V, Spangler R, Marshall D, McCauley S, Rodriguez HM, Oyasu M, *et al.* Allosteric inhibition of lysyl oxidase-like-2 impedes the development of a pathologic microenvironment. Nat Med 2010;16:1009–1017.
38. Lopez B, Querejeta R, Gonzalez A, Larman M, Diez J. Collagen cross-linking but not collagen amount associates with elevated filling pressures in hypertensive patients with stage C heart failure: potential role of lysyl oxidase. Hypertension 2012;60:677–683.
39. Chapman MA, Pichika R, Lieber RL. Collagen crosslinking does not dictate stiffness in a transgenic mouse model of skeletal muscle fibrosis. J Biomech 2015;48:375–378.
40. Maki JM, Rasanen J, Tikkanen H, Sormunen R, Makikallio K, Kivirikko KI, *et al.* Inactivation of the lysyl oxidase gene Lox leads to aortic aneurysms, cardiovascular dysfunction, and perinatal death in mice. Circulation 2002;106:2503–2509.
41. Weber MA, Nagel AM, Jurkat-Rott K, Lehmann-Horn F. Sodium (23Na) MRI detects elevated muscular sodium concentration in Duchenne muscular dystrophy. Neurology 2011;77:2017–2024.